

Article

Designing Isolation Valve System to Prevent Unexpected Water Quality Incident

Geumchae Shin [†], Soon Ho Kwon [†]  and Seungyub Lee ^{*} 

Department of Civil and Environmental Engineering, Hannam University, Daejeon 34430, Republic of Korea; geumchae1999@gmail.com (G.S.); rnjstnsgh90@gmail.com (S.H.K.)

* Correspondence: seungyub.lee@hnu.kr

[†] These authors contributed equally to this work.

Abstract: Designing an effective isolation valve system (IVS) is vital to enhance resilience against unforeseen failures in water systems. During isolation, the system's hydraulics undergo changes, potentially causing alterations in flow direction and velocity, leading to the dislodgement of accumulated materials and triggering unexpected water quality incidents. This study presents a novel IVS design approach by integrating the consideration of flow direction change (FDC) as an additional constraint within conventional reliability-based models. Two optimization models, Optimization I and Optimization II, prioritize reliability, with the latter also factoring in valve installation cost as a multi-objective function. Performance evaluation metrics, such as the Hydraulic Geodesic Index (HGI), Modified Resilience Index (MRI), and robustness index, were employed for a comprehensive analysis. The results indicated more than 40 instances of FDC in the traditional design, challenging the conventional notion that a higher number of valves inherently reduces risk. The superiority of the proposed model persisted for the single reservoir network in Optimization II. However, for networks with multiple reservoirs, the traditional design outperformed the proposed model, particularly in terms of cost. Nevertheless, when comparing designs with similar reliability, the proposed model showcased a superior performance, despite its higher associated cost. Notably, the proposed approach exhibits potential cost-effectiveness, considering the potential economic losses attributable to water quality incidents. In summary, the implementation of this methodology can effectively manage both water quality and quantity, enabling the identification of vulnerable pipes within the network for sustainable management.



Citation: Shin, G.; Kwon, S.H.; Lee, S. Designing Isolation Valve System to Prevent Unexpected Water Quality Incident. *Sustainability* **2024**, *16*, 153. <https://doi.org/10.3390/su16010153>

Academic Editor: Miklas Scholz

Received: 20 October 2023

Revised: 5 December 2023

Accepted: 20 December 2023

Published: 22 December 2023



Copyright: © 2023 by the authors. Licensee MDPI, Basel, Switzerland. This article is an open access article distributed under the terms and conditions of the Creative Commons Attribution (CC BY) license (<https://creativecommons.org/licenses/by/4.0/>).

Keywords: water quality failure; flow direction change; risk pipe; pipe failure; segment isolation

1. Introduction

The water distribution network (WDN) is a vital component that is responsible for delivering water to consumers while maintaining optimal pressure and water quality. Ensuring the functionality of the WDN is crucial for the sustainability of our society; however, the occurrence of abnormal conditions due to aging infrastructure or natural disasters poses a constant threat throughout its lifecycle [1]. In such instances, it becomes necessary to isolate the affected area using isolation valves for maintenance activities. Unfortunately, this isolation results in alterations to the WDN layout [2], inevitably changing the flow characteristics (velocity, flow rate, direction, etc.) across the network [3]. These changes in flow characteristics can temporarily reduce water flow and pressure, but more significantly, they may lead to unexpected water quality incidents [4,5]. For instance, South Korea faced a red water issue in 2019, primarily attributed to changes in flow direction resulting from alterations in water sources—an incident that could potentially occur due to valve operations [6].

As previously mentioned, valves within the WDN are crucial components facilitating the isolation of areas in need of recovery from abnormal conditions to ensure the sustainability of the system. The smallest isolatable unit through valve closure is commonly referred

to as a segment [7]. The determination of segments relies on valve locations, impacting the hydraulic characteristics (flow and pressure) and the potential damage incurred upon segment isolation. Given the impracticality of an experimental approach for determining valve locations, it becomes essential to estimate potential impacts using simulation tools, such as hydraulic models. Consequently, developing a methodology for segment identification and integrating it into hydraulic models to assess potential impacts and damaged areas is a key task in designing the isolation valve system (IVS). Numerous studies have proposed algorithms for segment identification [7–11].

Building on segment identification algorithms, subsequent studies have delved into assessing the potential impacts of IVS design by using various performance indicators, such as reliability [12,13], vulnerability [14,15], robustness [16], and resilience [17,18]. Recent contributions by Yang et al. [19] and Lee and Jung have introduced methodologies for the addition or removal of valves in pre-designed IVS or in a phased IVS design with network expansion considerations. While the potential for water quality incidents following valve operations has been acknowledged in several studies [3,20], there has been a notable gap in research directly addressing water quality concerns in IVS design. In contrast, instances of valve operation have seen consideration of water quality impacts. For example, Kang and Lansey [21] adjusted chlorine concentrations through chlorination facility and valve operations to enhance water quality management. Additionally, Brentan et al. [3] emphasized that flow paths and residence times change during valve operations for leakage and pressure management, emphasizing the need for valve operations that consider both hydraulic and water quality impacts simultaneously. Similarly, Dias et al. [22] confirmed that water quality deteriorates in specific areas due to prolonged residence times in accordance with the district metered area (DMA) configuration method. Although existing knowledge recognizes changes in water quality and flow characteristics based on valve locations, these factors have not been systematically considered in the IVS design stage.

As emphasized in various studies, alterations in flow characteristics resulting from valve closure can lead to common water quality issues, notably affecting chlorine concentration and turbidity [5,21,22]. A decline in chlorine concentration is often linked to extended residence times, with a higher likelihood of reduced concentration when the flow path deviates from its original configuration. Turbidity problems can manifest in various ways, primarily attributed to changes in flow velocity or alterations in flow direction within the pipeline [23,24]. Excessive flow velocity, particularly in pipes with low velocity during normal operation, can contribute to turbidity concerns. Flow direction changes, such as unexpected backflow in pipes with no usual directional alterations, can also induce turbidity. These characteristics are commonly leveraged in pipe-flushing practices, where specific velocities are induced for cleaning or reverse direction flow is employed to facilitate flushing [25,26]. Additionally, some WDNs are designed to generate a minimum velocity for daily flushing, defined as the self-cleaning velocity [4]. Methodologies presented in [5,27] outline approaches to secure self-cleaning velocities by adjusting network layout or modifying configuration through valve closure, respectively. However, pipes unable to achieve the self-cleaning velocity under normal conditions pose a potential risk of inadvertent turbidity issues following valve closure. Hence, the design of IVS should incorporate considerations of hydraulic characteristics [28].

This study introduces a novel IVS design approach aimed at minimizing inadvertent water quality failures resulting from segment isolation. The key innovation lies in incorporating the flow direction change (FDC) as an additional constraint to traditional reliability-based IVS design models. Two optimization models, based on the genetic algorithm (GA) and Non-Sorted Genetic Algorithm-II (NSGA-II), are developed with these constraints. In the single-objective model (Optimization I), reliability serves as the objective function, while the multi-objective model (Optimization II) factors in both reliability and valve installation cost. The EPANET model, employing a pressure-driven analysis (PDA) algorithm [29], is utilized to determine reliability and flow direction. The proposed models are tested on a hypothetical grid network and two benchmark networks (Austin

and Pescara networks), and their performance is assessed by comparing the results against those obtained through traditional design approaches.

2. Methodology

The objective of this study is to propose an optimal IVS design approach considering the FDC, thereby enhancing traditional IVS design methods by reducing potential risks to water quality. Note that while various factors can lead to water quality failures, we specifically concentrate on failures resulting from the detachment of deposits (e.g., discoloration). We opted for the reliability-based design method, commonly employed in traditional approaches, and conducted a comparative analysis between designs with and without FDC consideration. The optimization model encompasses two distinct models: GA for single-objective optimization (maximizing reliability) and NSGA-II for multi-objective optimization (maximizing reliability and minimizing installation cost). In both optimization techniques, FDC is incorporated as a constraint to address the risk of water quality incidents, while the single-objective model includes the number of valves installed as an additional constraint. Furthermore, the Hydraulic Geodesic Index (HGI) [30], robustness index [31], and modified resilience index (MRI) [32] were employed to assess the performance of the proposed approach. This section provides a detailed description of potential water quality risks, optimization models, and performance evaluation metrics (Figure 1).

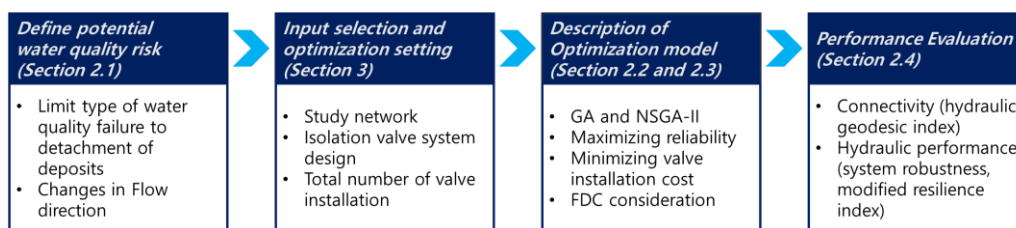


Figure 1. General procedure of this study.

2.1. Potential Water Quality Risks

The detachment of deposited scale within the pipe is a direct cause of water quality failures. It can occur due to various reasons, for example, a change in water flow due to different situations, such as emergency water transfer, sudden valve operation, or pipeline replacement. However, most of those scenarios can be categorized as sudden changes in velocity or flow direction.

Generally, velocity criteria encompass the self-cleaning velocity under normal operating conditions and the minimum flushing velocity. These criteria are closely related to the velocity at which deposits can be detached from the pipes [4,6,33]. The recommended range for self-cleaning velocity is typically 0.2–0.4 m/s [5,34,35], while a flushing velocity of 0.9 m/s or higher is generally suggested [6,33]. Various velocity criteria have been proposed, with variations depending on circumstances and the condition of existing pipes and networks. However, these criteria carry uncertainties, as described by Van Den Boomen et al. [4]. Their experimental study revealed that changes in velocity have a greater potential to detach deposited scale than the actual minimum velocity requirement.

On the other hand, changes in flow direction have a higher likelihood of causing water quality incidents compared to velocity criteria, as reported in the literature [24,25,27,36]. For instance, studies by Ahn et al. [36] and Armand et al. [37] indicated that backward flows are more efficient in suspending deposits or cleaning pipes compared to simple velocity changes. Similarly, when there is a change in flow direction within the pipe, it directly affects the detachment of previously stabilized scale [24,33]. In other words, changes in flow direction have a higher potential to lead to water quality failures compared to changes in velocity.

Given this, the FDC, which measures the frequency of changes in flow direction for each pipe during specific scenarios, is selected to consider potential water quality failures.

In this context, scenarios correspond to the isolation of segments. Specifically, FDC is determined by counting pipes experiencing changes in flow direction before and after sequentially isolating each segment based on IVS design. The FDC is determined in two steps: first, the flow directions of all pipes before isolation are identified by hydraulic analysis; and then, by isolating each segment, the flow direction is evaluated per pipe. If a certain pipe experiences changes in flow direction before and after isolation, the number of changes in flow direction is counted to finalize the FDC.

2.2. Segment Identification

To explore segments and determine optimal valve locations, various studies have proposed segment identification methods [7–11]. Typically, these studies transformed the WDN into a graph representation to differentiate segments. The algorithm employed in this study, proposed by Jun and Loganathan [8], also creates three matrices for segment identification. These matrices are (1) the Node-Arc matrix, which stores information about the connectivity between nodes and pipes; (2) the Valve Location Matrix, recording valve locations; and (3) the Valve Deficiency Matrix, indicating potential valve locations between nodes and pipes where valves are not located. All three matrices have dimensions corresponding to the number of nodes and pipes and store either “1” or “0” based on the connectivity or presence (“1” if connected or present; “0” otherwise).

It is important to note that the Valve Location Matrix can only have “1” value where Node-Arc Matrix is also “1” (indicating that a certain node and pipe are connected to each other). Furthermore, the Valve Deficiency Matrix should be “1” where Node-Arc Matrix is “1” but the Valve Location Matrix is “0” (indicating that a valve can be installed but is not currently installed).

The algorithm by Jun and Loganathan [8] performs iterative row-wise and column-wise searches until segments are identified. Figure 2 illustrates this procedure, demonstrating the process of finding a segment starting from N1. For instance, beginning from node N1, a row-wise search is conducted and identifies two “1”s in P1 and P3. Subsequently, a column-wise search is performed from P1 and P3 to identify the next component in the segment. While P1 does not have any “1”s in the column, ending search for the P1 column, P3 column has a “1” in N3. Consequently, a subsequent row-wise search is conducted to identify any “1” in the row. However, as no more “1”s are present in N3 row, the search for N1 is terminated, and N1, N3, P1, and P3 are identified as the first segment. This procedure is repeated for all nodes until either the last node or all nodes are assigned to segments, at which point the process terminates. For more detailed information, please refer to Jun and Loganathan [8]. In this study, the Valve Location Matrix is constructed during the design process, meaning that the Valve Location Matrix is determinant.

2.3. Optimization Model

The IVS design incorporates two distinct optimization models for determining optimal valve locations: one utilizing a GA, referred to as Optimization I; and the other employing NSGA-II, denoted as Optimization II. Both optimization models share a common objective function, focusing on reliability (F_1), with the FDC considered a constraint. Furthermore, Optimization I introduces the number of valve installations as an additional constraint, while Optimization II integrates valve cost as an extra objective function. The summary of objective functions and constraints for each optimization model is presented in Table 1.

In Table 1, Rel_{Avg} represents the average reliability, which is the average value of reliability calculated for each segment isolation with consideration of segment isolation probability. C_{Val} is cost of valve installation ($C_{Val} = 701.49e^{7.7D_i}$, where D_i is diameter of i -th valve) [38] and serves as the second objective function (F_2) for Optimization II. Note that the unit was exchanged from EUR to USD based on the average exchange rate of 2019. FDC is total number of changes in flow direction of pipes following segment isolation, distinguishing this approach from the traditional IVS designs. N_{Val} is the number of valve installations, and $N_{Val,tot}$ is the total number of valves that can be installed in the WDN,

equivalent to twice the number of pipes. Lastly, α is a ratio ranging between 0 and 1.0. N_{val} introduces an additional constraint solely in Optimization I, instead of being part of F_2 , to eliminate the influence of cost deviation, representing the total number of valves that can be installed. Reliability is defined as the ratio of delivered demand (demand output of EPANET) to required demand (base demand input of EPANET). Equations (1)–(4) outline the formulas for calculations.

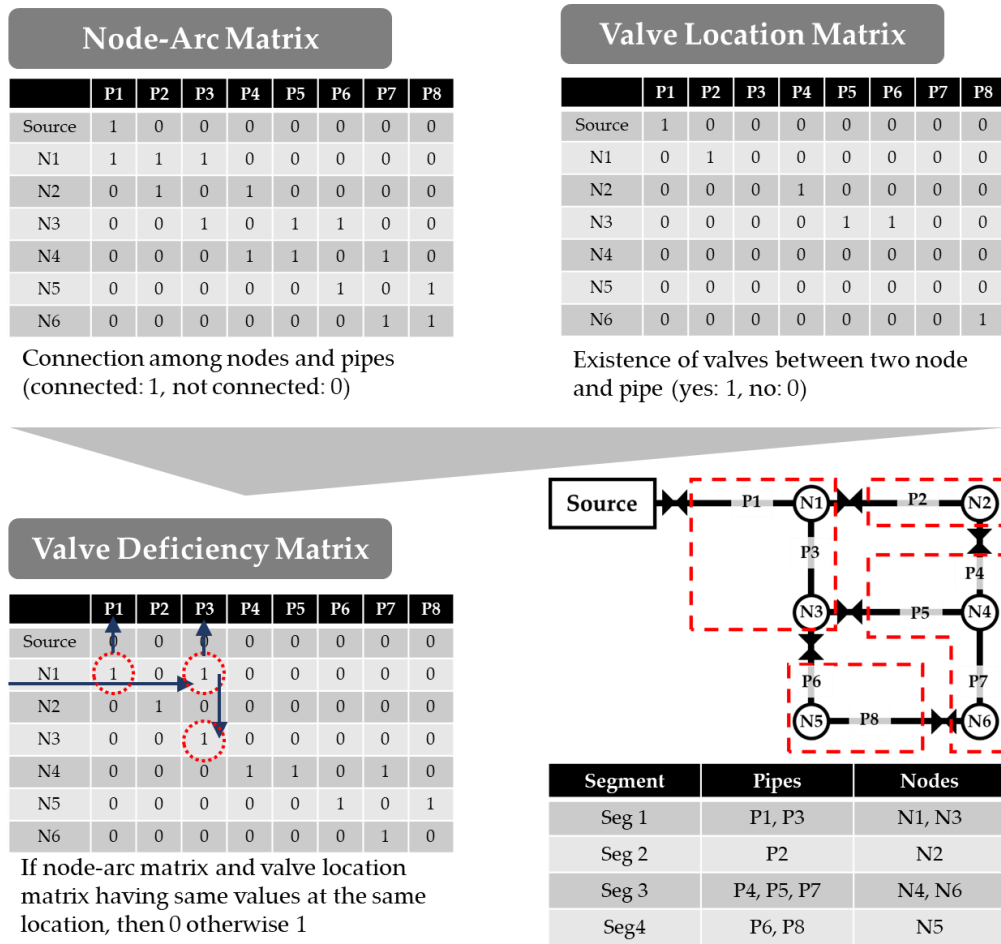


Figure 2. Description of valve identification algorithm.

Table 1. Objective functions and constraints for each optimization model.

Optimization Model	Objective Function	Constraints
I	$F_1 = \max(Rel_{Avg})$	$FDC = 0$ $N_{val} = \alpha \times N_{val,tot}$
II	$F_1 = \max(Rel_{Avg})$ $F_2 = \min(C_{Val})$	$FDC = 0$

$$Rel_{Avg} = \frac{\sum_{s=1}^{NSegment} p_{segment,s} \times rel_s}{\sum_{s=1}^{NSegment} p_{segment,s}} \tag{1}$$

$$rel_s = \frac{\sum_{j=1}^{nnodes} Q_{avi,j}}{\sum_{j=1}^{nnodes} Q_{reg,j}} \tag{2}$$

$$p_{segment,s} = \sum_{i=1}^{n_{pipe_segment}} p_{pipe,i} \quad (3)$$

$$p_{pipe,i} = 1 - e^{-r_i L_i} \quad (4)$$

where $p_{segment,s}$ represents the probability of the s -th segment isolation, calculated as the sum of individual breakage probabilities for pipes included in the segment; rel_s represents the reliability during segment isolation; $N_{Segment}$ is the total number of segments; n_{nodes} is the total number of demand nodes; $Q_{avi,j}$ represents the actual demand based on pressure; and $Q_{reg,j}$ represents the required demand. And $n_{pipe_segment}$ represents the number of pipes included in the segment, $p_{pipe,i}$ represents the breakage probability for the i -th pipe, r_i represents the breakage rate per length (breaks/ft) for the i -th pipe given by Su et al. [39], and L_i represents the length of the i -th pipe (ft). For the entire analysis, the PDA was conducted to address any unmet demand resulting from violations of minimum pressure standards and isolation from the source [40]. Furthermore, the calculation of reliability is iteratively performed for each segment isolation until all segments are evaluated.

2.4. Performance Evaluation

In this study, various performance indicators were considered to compare the performance of the traditional design with that of the proposed design. Firstly, as isolation results in disconnection, we evaluated a surrogate measure of connectivity, specifically the HGI [30]. Comparing HGI allows us to assess whether all demand nodes remain connected to the water source or not. Additionally, the system robustness index [31] and MRI [32] were employed to evaluate the endurance of the WDN during isolation.

2.4.1. Hydraulic Geodesic Index (HGI)

In the case of WDNs, which exhibit a geometric shape similar to graphs, graph theory has been frequently employed for analyzing nodal connectivity. In this study, to examine the characteristics of design alternatives with or without considering FDC, we utilized the HGI proposed by Lee and Jung [30], which is based on graph theory. HGI quantifies the connectivity between the water source and each demand node, emphasizing the connectivity among various nodes rather than the overall connectivity. It indirectly reflects energy loss. In other words, demand nodes with a high HGI have a short hydraulic distance from the water source and experience low energy loss. HGI is based on a directed-weighted graph, with the weights being the resistance coefficients used in EPANET to calculate energy loss. Equation (5) represents the calculation of the HGI.

$$w_i = 4.727(\text{norm}C_i)^{-1.852}(\text{norm}D_i)^{-4.871}(\text{norm}L_i) \quad (5)$$

where w_i represents the weight of the i -th pipe, C_i represents the roughness coefficient of the i -th pipe, D_i represents the diameter of the i -th pipe, and L_i represents the length of the i -th pipe. The term “norm” indicates normalization, which is calculated based on the maximum value of each variable. HG can be defined as the sum of the weights of the pipes included in the minimum path determined by Dijkstra’s shortest-path algorithm, considering the weights from the nearest water source to each demand node. HG is not normalized and can sometimes yield very large values, which may not provide intuitive results, as higher values indicate lower connectivity with the water source. In addition, HG does not intuitively represent connectivity, as smaller values indicate higher connectivity. Therefore, HG undergoes a min–max normalization process to obtain values between 0 and 1. The normalized values of HG for each demand node (represented as k) are defined as HGI , and the Equation (6) represents this normalization process.

$$HGI_k = \frac{1}{(HG_k / \text{min}HG)} \quad (6)$$

where $minHG$ is the shortest value among all k -th demand nodes' HG (HG_K) in the WDN and is considered for min–max normalization. Note that, HGI_k ranges from 0 to 1, with values closer to 1 indicating stronger connectivity. In this study, the purpose is to understand the variation in HGI_k before and after segment isolation in the design alternatives. Therefore, to assess the variation in $HGI_{k,s}$, another normalization was applied, and the baseline (HGI_k) for normalization was the HGI at each node in the steady state without segment isolation (Equation (7)).

$$normHGI_{k,s} = \frac{HGI_{k,s}}{HGI_k} \quad (7)$$

In the above equation, s represents the segment isolation scenario. Therefore, $normHGI_{k,s}$ represents the normalized HGI at the demand node under the segment isolation scenario. Lastly, the average value of $normHGI_k$ for each demand node is defined as the normalized system HGI ($normSHGI$), which can be calculated as follows:

$$normSHGI = Avg(normHGI_k) \quad (8)$$

2.4.2. System Robustness Index (sysRob)

In addition, for the comparison of the final results, this study considered a system robustness index ($sysRob$) proposed by Jung et al. [31] which is basically the coefficient of variation in pressure. Before calculating the $sysRob$, the robustness index of each demand node should be identified. The general formula for representing the robustness index is given as follows.

$$Rob_i = 1 - \frac{\sigma_{P_i}}{P_{avg_i}} \quad (9)$$

where σ_{P_i} represents the standard deviation of pressure at i -th node, and P_{avg_i} is average pressure of i -th node. The final robustness index is calculated as the minimum value among the calculated Rob_i values for each demand node selected. This can be expressed as follows:

$$sysRob = min(Rob_i) \quad (10)$$

2.4.3. Modified Resilience Index (MRI)

In this study, the MRI proposed by Jayaram and Srinivasan [32] was applied to compare the performance between two different design approaches. The MRI is the revised version of the Resilience Index that originated from Todini [41]. The revision was made to make the index more applicable to the WDN with multiple reservoirs by only considering the total energy surplus at the demand nodes (Equation (11)). A larger MRI value indicates a larger amount of energy surplus at the demand nodes and, thereby, the greater resilience of the WDN.

$$MRI = \frac{\sum_{i=1}^n q_i^* (h_i - h_i^*)}{\sum_{i=1}^n q_i^* h_i^*} \quad (11)$$

3. Study Networks

In this study, we applied the proposed models to three networks: one hypothetical network (grid network) and two benchmark networks (Austin and Pescara) (Figure 3). These networks were mainly selected due to their differences in the number of reservoirs. Note that Figure 3 also displays the flow directions of each pipe under normal operation.

The grid network consists of a total of 61 pipes with the same diameter (1000 mm). It supplies a demand of 3409 L per second (lps) to 36 demand nodes, using gravity from a single water source at an elevation of 80 m. The demand is uniformly distributed to all nodes, and the minimum required pressure is set to 30 m. There are overall 61 pipes. The Austin network is a medium-sized WDN consisting of 2 reservoirs, 67 nodes, and 91 pipes. The minimum allowable pressure requirement was 28 m. The diameter of

91 pipes ranges from 0.152 mm to 1.829 mm. The overall demand of 762.2 lps is supplied by two reservoirs, with water from reservoir 1 being lifted through a pump station (total 7 pumps), and with water from reservoir 2 (lower right reservoir) being supplied via gravity. The Pescara Network consists of 3 reservoirs, 99 pipes, 71 nodes, and a total system demand of 498.28 lps. The diameters of pipes vary between 100 mm to 400 mm. All three reservoirs supply water via gravity, with the minimum required pressure set to 30 m.

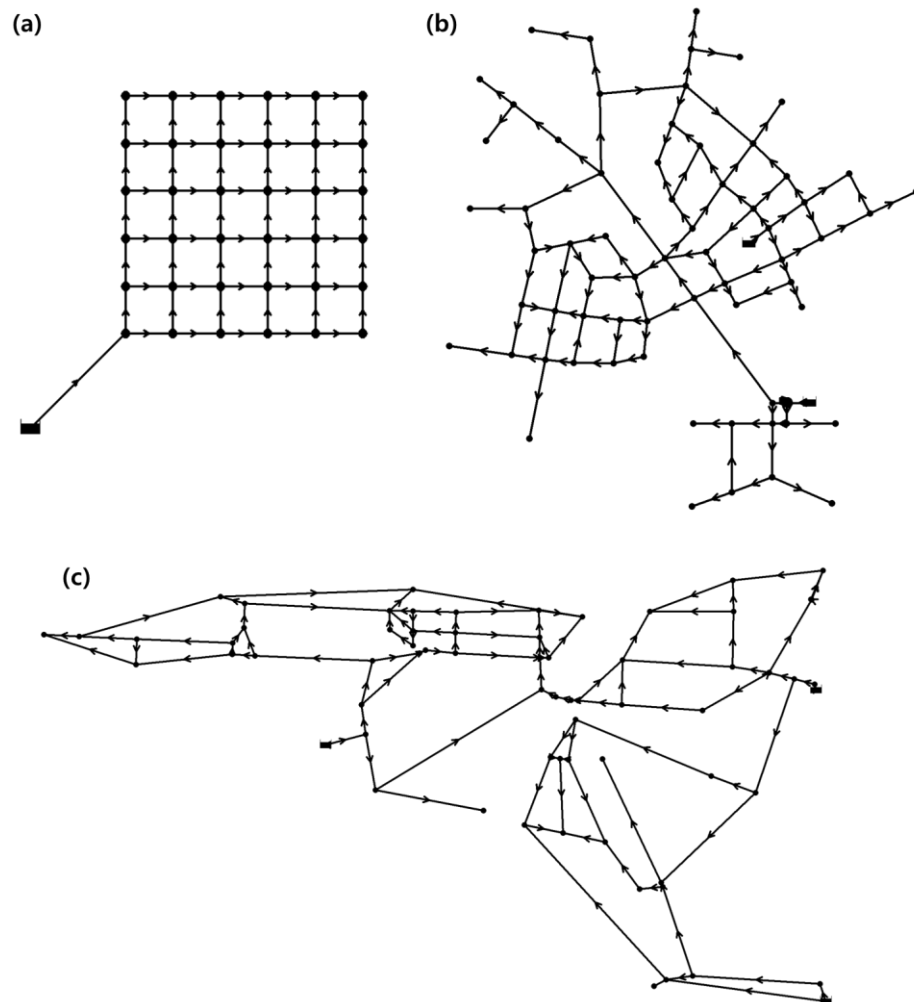


Figure 3. Schematics of study networks. (a) grid network, (b) Austin network, and (c) Pescara network.

We conducted IVS designs with and without considering the FDC as a constraint in traditional reliability-based design. We compared the two design approaches to analyze the characteristics of each design approach based on the performance evaluation metrics described in Section 2.4. Furthermore, the trade-off between cost and reliability is examined for both design approaches.

For Optimization I, it is only applied to the grid network, while for Optimization II, it is applied to all three networks. For Optimization I, the number of valves (N_{val}) was constrained to be between 30% and 70% of the total possible valve installations (up to 2 per pipe; a maximum of 122 valves) to exclude cost deviations during optimization (meaning α is 0.3 to 0.7 in increments of 0.1). Each valve installation is defined as V30 to V70. For Optimization II, both reliability and cost were applied as objective functions. Moreover, for Optimization II, the optimization approach considering FDC is defined as the proposed design, and the approach not considering FDC is defined as the traditional design.

4. Application Results and Discussion

4.1. Optimization I

The optimization results are summarized in Table 2. Scenarios are distinguished as V30 to V70 based on the number of installable valves (α is 0.3 for V30 and increments by 0.1), and “−1” (considering FDC; proposed design) or “−2” (not considering FDC; traditional design) is used to differentiate scenarios depending on whether FDC is considered. The results show that, regardless of the number of valves, designs that do not consider FDC result in higher occurrences. It is worth noting that a higher number of flow direction changes generally indicates a higher risk of water quality incidents. However, even a single occurrence of FDC can lead to critical water quality incidents, making their occurrence or absence an important consideration.

Table 2. Summary of Optimization I results for all valve installation scenarios.

Scenario	Rel_{Avg}	FDC	$norm$ $SHGI$	$sysRob$	Avg MRI	Avg Shortage	SD * Shortage
V30-1	0.893	0	0.859	0.579	−0.375	480.26	825.16
V30-2	0.898	42	0.857	0.550	−0.565	480.26	819.71
V40-1	0.925	0	0.918	0.688	0.035	280.15	663.17
V40-2	0.931	46	0.915	0.675	−0.037	281.66	660.18
V50-1	0.942	0	0.945	0.745	0.224	186.69	562.53
V50-2	0.950	46	0.940	0.702	−0.042	198.08	563.31
V60-1	0.948	0	0.957	0.763	0.262	146.78	532.75
V60-2	0.961	56	0.952	0.744	0.146	150.43	518.29
V70-1	0.953	0	0.966	0.780	0.314	115.29	501.07
V70-2	0.967	70	0.963	0.777	0.271	116.37	459.81

* Standard deviation.

Looking at the overall frequency of FDC, we can see that it was not always the case that a larger number of valves resulted in lower risk. This indicates, as mentioned in the study by Fiorini Morosini et al. [42], that having a large number of valves may not necessarily be advantageous in maintaining the functionality of a real WDN. Additionally, it suggests that there may be a higher likelihood of water quality incidents in networks with a greater number of valves, according to the existing designs.

In most cases, FDC was observed in the top-left or bottom-right pipes (Figure 4). This is mainly because of the difficulties in securing flow direction in those areas. As all pipe characteristics are identical for the grid network, the general direction of flows is in an upward direction and left to right. And when any of the nodes in the gray dotted lines are isolated, there is a higher chance of having reverse-direction flow for the top-left or bottom-right pipes. Figure 5 illustrates the optimal valve positions for design scenarios V60-1 and V60-2.

In Figure 5, it can be observed that, in the design considering FDC (V60-1), valves are installed at both the leftmost and bottommost junctions. As discussed earlier, in the left-most junctions, flow always occurs toward the right, and in the bottommost junctions, flow occurs toward an upward direction. Therefore, in the design considering FDC (V60-1), valves are installed in these pipes to control reverse flow. However, this generally includes demand nodes as well, eventually leading to lower reliability or higher shortage. In contrast, in the design not considering FDC (V60-2), there are no valves in these pipes, meaning that reverse flow cannot be controlled during the isolation of specific segments. For example, the gray dotted box with a star represents some segments that do not include demand nodes but result in reverse flow for pipes supplying water to the node located above the segments on the left side of the network and the node located on the right side of the segment for the lower-side segment. However, in this case, no demand nodes are actually isolated from the source, resulting in less shortage or higher reliability compared to the design considering FDC, as evaluated in Table 2.

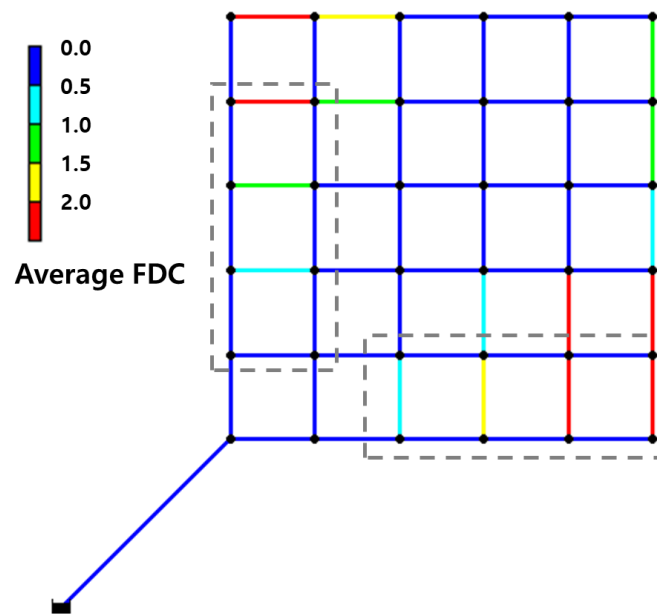


Figure 4. Average FDC result of Optimization I (V30-2 to V70-2; not considering FDC case).

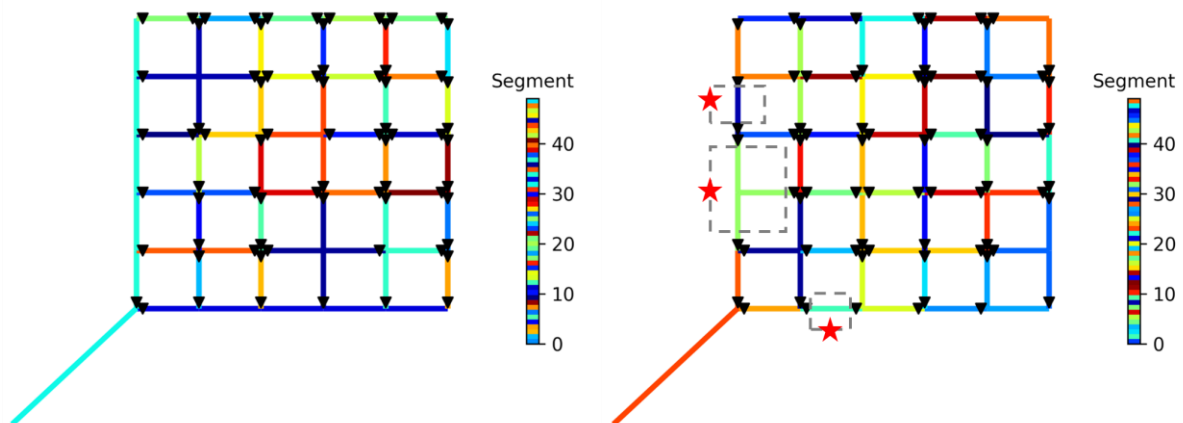


Figure 5. Valve locations of V60-1 and V60-2.

Figure 6 illustrates the percentage difference in average pressure and average HGI between V60-1 and V60-2. Note that a higher value indicates that V60-1 is in a better state. The results in Figure 6 show that V60-1 maintained pressure well compared to V60-2 in general. This is also reflected in the system robustness results shown in Table 1. However, the HGI results show that V60-2 is generally higher compared to V60-1, in contrast to the results shown in Table 1. As previously mentioned, HGI quantifies the minimum hydraulic distance from the nearest source to a specific demand node. A decrease in HGI implies that the path to the same demand node has become longer compared to the original route, indicating that changes in flow paths result in pressure reductions or variation. Therefore, when a specific demand node is not isolated from the source, there are higher chances for the demand node to be connected to the source in the shortest path (or efficiently). In other words, V60-1 should have a higher HGI than V60-2. The main reason that V60-2 had a higher average HGI for each node was because of its design nature to minimize node isolation. As shown in Figure 5, V60-2's design tends to exclude demand nodes for isolation to increase reliability due to isolation, while V60-1 typically includes demand nodes to eliminate FDC. And when a certain demand node is isolated from the source, the HGI for the demand node is zero. This leads to a lower average HGI. If those isolated

demand nodes are excluded from the average calculation, then V60-1 always maintains identical HGI for all demand nodes, indicating that all demand nodes are connected with the source in the shortest pathways if they are not disconnected from the source.

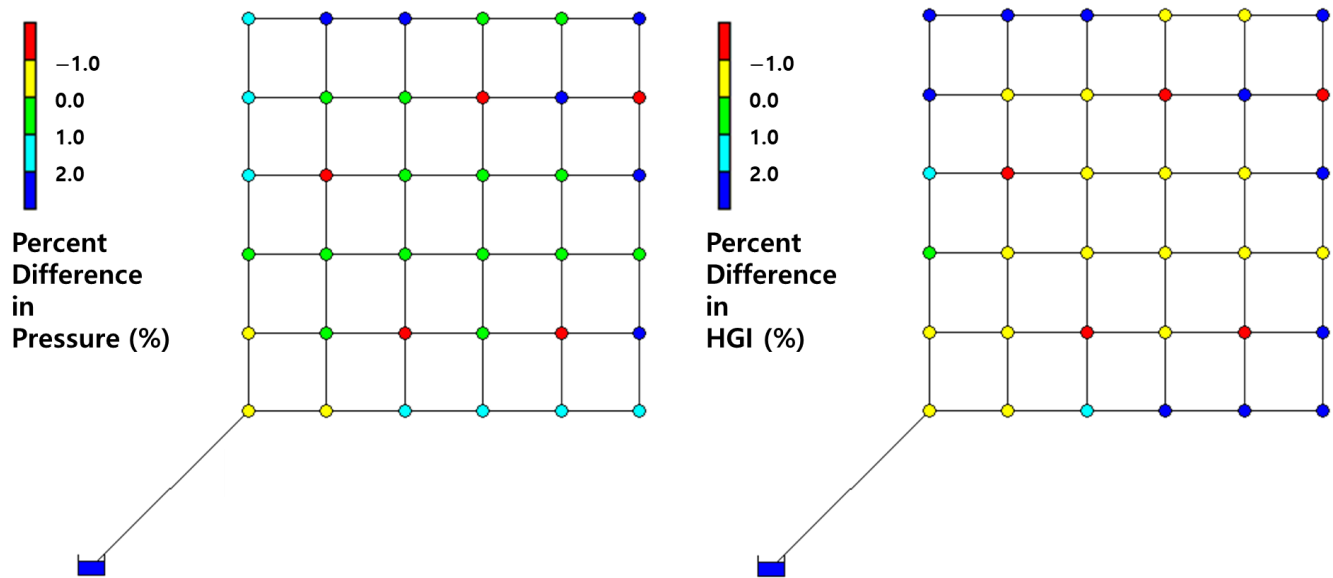


Figure 6. Percent difference in pressure and HGI of V60-1 and V60-2.

In summary, considering the FDC for IVS design may reduce the performance of the system at a glance. However, the amount of difference is not significant, considering the benefit of preventing potential water quality incidents. This suggests that considering FDC in the design not only reduces the risk of water quality incidents but also maintains the network's performance even in cases of specific segment isolation compared to traditional design.

4.2. Optimization II

The multi-objective optimal design of IVS in Optimization II selects representative results from the Pareto front, using two different criteria: (1) based on similar cost and (2) similar observed reliability. The summarized outcomes can be found in Table 3.

Upon comparison, the traditional design outperformed the proposed design when considering similar costs. The assessment of reliability between the two design models showed that networks with multiple reservoirs exhibited larger performance gaps. In the case of a single-reservoir grid network, most performance metrics, except for reliability, favored the proposed design. This suggests that the proposed design can effectively be implemented in single-reservoir networks to minimize flow directional changes, while maintaining overall performance.

However, for networks with multiple reservoirs, such as the Austin and Pescara networks, the performance disparities between the two design models increased. Generally, networks with multiple reservoirs are more likely to experience changes in flow directions, especially when one of the reservoirs is isolated. For example, in the optimal design results for the Austin network with similar costs (Figure 7), the pipes within the red dotted rectangular area in the proposed design (Figure 7a) constitute the backbone of the network, transporting water from the lower-side reservoir to the upper area. By isolating these pipes, water flow from the upper-side reservoir to the lower area is disrupted, effectively eliminating flow direction changes. In all proposed design cases, one of the segments encompasses all the pipes in the red dotted rectangular area that supply water from the lower-side reservoir to the upper area of the network. However, if a portion of the pipes in this area is isolated, there is a higher likelihood of experiencing reverse flow. For instance, if

the pipe within the red dotted rectangular area in Figure 7b is isolated, the pipe highlighted with a star symbol in Figure 7b would experience reverse flow.

Table 3. Summary of Optimization II results for all valve installation scenarios. Note that, in regard to the scenario, (1) is a similar C_{Val} comparison, and (2) is a similar Rel_{Avg} comparison. Also, G is grid network, A is Austin network, P is Pescara network, O indicates proposed design (considering FDC), and X indicates traditional design (FDC not considered).

Scenario		N_{Val}	C_{Val}	Rel_{Avg}	FDC	$normSHGI$	$sysRob$	Avg MRI	Avg Shortage	SD * Shortage	
(1)	G	O	93	144,069,465	0.956	0	0.971	0.834	0.315	100.38	482.29
		X	93	144,069,465	0.970	50	0.968	0.773	0.294	102.35	471.44
	A	O	60	949,219	0.870	0	0.897	0.328	0.094	551.88	1343.06
		X	65	943,002	0.928	86	0.925	0.692	0.091	398.24	1004.50
	P	O	38	69,920	0.763	0	0.895	0.516	-0.019	42.86	99.09
		X	39	69,718	0.919	158	0.891	0.586	-0.039	43.44	57.75
(2)	G	O	93	144,069,465	0.956	0	0.971	0.834	0.315	100.38	482.29
		X	62	96,046,310	0.956	44	0.943	0.726	0.307	187.09	546.52
	A	O	60	949,219	0.870	0	0.897	0.328	0.094	551.88	1343.06
		X	63	634,926	0.880	46	0.909	0.276	0.093	474.48	1278.97
	P	O	38	69,920	0.763	0	0.895	0.516	-0.019	42.86	99.09
		X	29	46,324	0.819	52	0.858	0.409	-0.030	60.72	70.10

* Standard deviation.

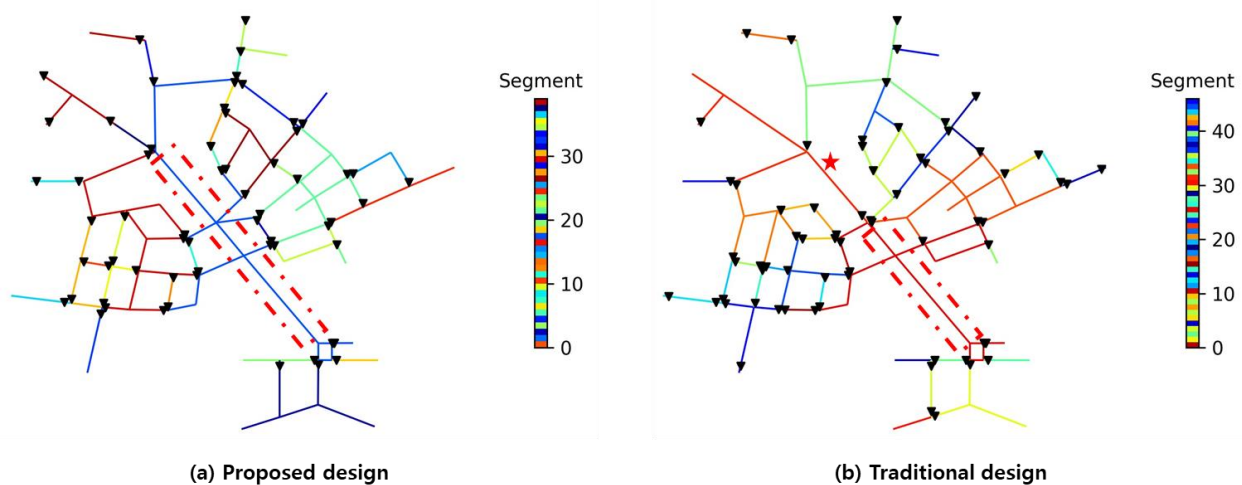


Figure 7. Optimal design results of similar cost for Austin network.

However, the segment that includes the red dotted rectangular area in the proposed design (Figure 7a) eventually isolates the left part of the network, leading to increased water shortages. Consequently, the proposed design demonstrated lower reliability, $normSHGI$, and system robustness compared to the traditional design. The decrease in $normSHGI$ values was influenced by a factor similar to that observed in Optimization I, where nodes were more likely to be isolated to minimize changes in flow direction. This outcome resulted from the consistent connection of nodes to the reservoir via the shortest pathways, as evidenced by the higher average MRI values associated with the proposed design.

In scenarios where the two design models exhibited similar reliability, the proposed design showcased a superior performance, albeit at a higher cost (approximately 50% more). Directly comparing the benefits of reduced water quality failure incidents is challenging.

The economic losses from water quality failure may include revenue loss due to water supply disruptions, the identification and management of water quality failures, and insurance costs related to consumer sickness or fatalities [43]. Indirect costs also encompass healthcare expenses, increased strain on local medical facilities, and loss of productivity for affected individuals and families, among other considerations. The medical and productivity costs linked to a single water quality failure event can be substantial, as exemplified by the estimated costs of the *Cryptosporidium* outbreak in Milwaukee, Wisconsin, in 2003, totaling approximately USD 31.7 million and USD 64.6 million, respectively [44]. Furthermore, a reported expenditure of around USD 27.2 million for compensation in a previous red water incident, in 2019, in South Korea highlights the complexity of determining the precise economic value of water quality incidents. Even though a single event can lead to significant financial losses, the proposed design model may prove to be more cost-effective in certain cases. Additionally, in addition to reliability, the proposed design outperforms the alternative in various other aspects, suggesting that it may provide superior solutions not only for water quality incidents but also for quantity management.

Figure 8 illustrates the Pareto fronts of all the results, showcasing a trade-off between cost and reliability in both designs. However, as the number of reservoirs increases, a significant gap between the Pareto fronts becomes evident. Furthermore, the Pareto fronts of the proposed design are positioned at the tails of the traditional design, indicating the overall superiority of the traditional design in terms of reliability. Ultimately, the growing number of reservoirs implies inherent limitations in preventing flow directional changes due to segment isolation.

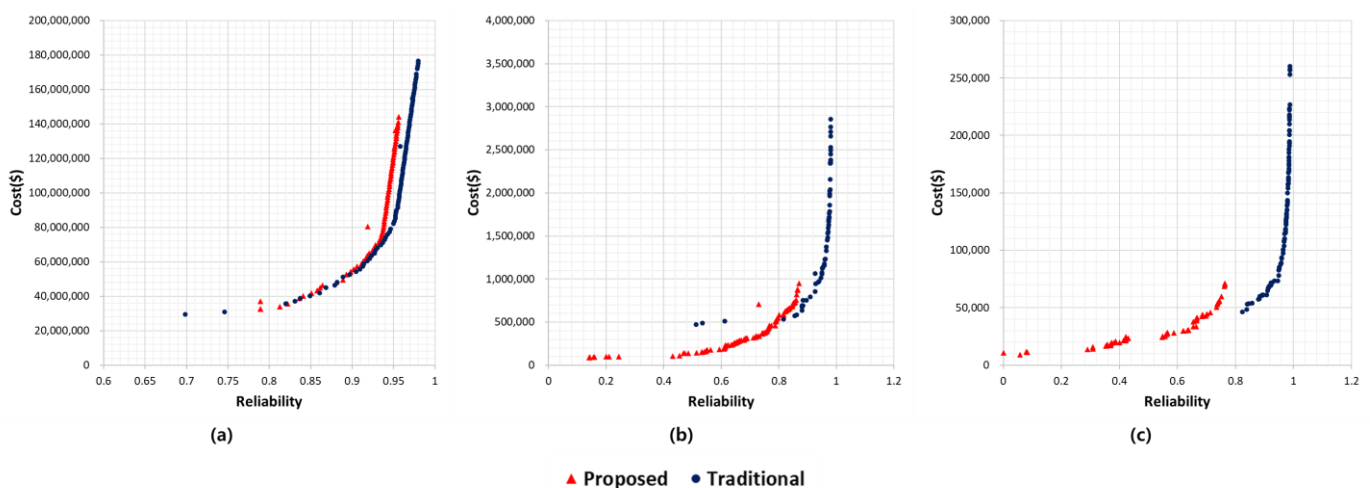


Figure 8. Pareto front results for all networks: (a) grid network, (b) Austin network, and (c) Pescara network.

It is worth noting that an additional cost of approximately 50% is required to prevent directional changes while maintaining a similar performance. If the budget allows or alternative methods for preventing water quality incidents are not feasible, designing the IVS with minimized directional changes can be considered. However, in cases where the budget is limited or other management methods, such as flushing or different practices for preventing water quality incidents, are available, allowing directional changes for certain easily manageable pipes may be advantageous. Especially in scenarios with a high number of reservoirs, focusing more on identifying pipes for concentrated management rather than completely eliminating directional changes may be more practical.

5. Conclusions

In this study, a novel approach to IVS design, aimed at minimizing unintended water quality failures, was proposed by integrating the FDC as an additional constraint in tradi-

tional reliability-based models. Two optimization models, Optimization I and Optimization II, were developed. Optimization I focuses on a single objective, prioritizing reliability, while Optimization II considers both reliability and valve installation cost as multi-objective functions. The FDC was incorporated as a constraint in both optimization techniques to assess the potential risk of water quality incidents, with additional constraints introduced for the single-objective model, including the number of installed valves. Performance evaluation metrics were employed to assess the efficacy of the proposed approach. The proposed approach was applied to a hypothetical grid network and two benchmark networks, allowing for a comprehensive evaluation compared to conventional design methodology.

Regarding the results of Optimization I, the traditional design exhibited over 40 FDC instances regardless of the number of installed valves, challenging the assumption that a larger number of valves inherently reduces risk. Generally, the proposed model prioritizes the inclusion of demand nodes within segments to eliminate flow directional changes, while the traditional model tends to exclude demand nodes to enhance reliability. Moreover, the proposed model's average pressure, HGI, and MRI results align closely with or slightly surpass those of the traditional model. Therefore, despite potentially compromising the initial performance, FDC, when considered in the design, not only reduces the risk of water quality incidents but also effectively maintains the network's overall performance.

Optimization II's results also show that the proposed design can be effectively applied for networks with a single reservoir, while networks with multiple reservoirs pose a bit more of a challenge. Especially when comparing results between two design approaches with similar costs, the traditional design outperformed the proposed design. However, when comparing designs with similar reliability, the proposed design displayed a superior performance despite coming with a higher cost. Directly comparing the benefits of reduced water quality incidents posed a challenge, but the proposed design may be more cost-effective considering potential economic losses due to a single water quality failure.

The main contribution of this study is the introduction of a consideration of directional factors that were previously overlooked in IVS design. The results indicate two main points. Firstly, in cases where there is only one reservoir, the proposed methodology can be applied with relative ease. With a single reservoir, the likelihood of reverse flow due to hydraulic transitions is low, making it possible to effectively install valves for sufficient water quality and quantity management. Secondly, in the case of multiple water sources, the model proposed in this study could be used to identify pipes vulnerable to water quality incidents based on the existing design. Additionally, depending on the situation, allowing directional changes in certain pipes and focusing on their concentrated management could help prevent water quality incidents in advance.

However, there are some remaining issues that can be tackled in the future. First, operational conditions can be included for analysis by applying an extended-period simulation. In this study, single-period simulations were conducted, assuming that no directional changes occur in the normal state. However, in reality, certain pipes, especially those associated with tanks, may undergo continuous directional changes even in the steady state. When designing using the model proposed in this study for such pipes, it would be possible to designate them as exceptional pipes for directional changes, considering them to be lower-risk pipes even in cases of directional changes leading to potential water quality incidents.

Second, the criteria for selecting risk-prone pipes for water quality incidents could be based not only on directional changes but also on practical pipe characteristics (diameter, length, aging, etc.) and operational conditions. It is important to note that water quality incidents can be caused by factors other than directional changes. For instance, as explored in Section 2.1, accidents can also occur due to velocity fluctuations, so it is essential to consider aspects beyond just directional changes. Also, transient scenarios are another important aspect to consider. Such considerations can provide additional insights into risk pipe evaluations.

Lastly, even though the proposed design is not very effective when the network has multiple reservoirs, the proposed design can provide valuable insights to manage the network to prevent water quality failure. Specifically, the evaluation of the impact of existing valve positions and the application of the methodology for preventing unexpected water quality incidents when adding new valves in the future can be areas of potential research.

Author Contributions: Conceptualization, G.S., S.H.K. and S.L.; methodology, S.L.; software, G.S. and S.H.K.; validation, S.L. and S.H.K.; formal analysis, G.S. and S.H.K.; investigation, S.H.K.; resources, S.L.; data curation, G.S. and S.H.K.; writing—original draft preparation, G.S.; writing—review and editing, S.L.; visualization, S.H.K.; supervision, S.L.; project administration, S.L.; funding acquisition, S.L. All authors have read and agreed to the published version of the manuscript.

Funding: This work was supported by the National Research Foundation of Korea (NRF) grant funded by the Korean government (MSIT) (No. NRF-2021R1C1C2004896).

Data Availability Statement: The data presented in this study are available upon request from the corresponding author. The data are not publicly available due to Security issue.

Conflicts of Interest: The authors declare no conflicts of interest.

Abbreviations

α	a ratio between 0 and 1.0
C_{val}	valve installation cost
C_i	roughness coefficient of the i-th pipe
D_i	diameter of the i-th pipe
FDC	total number of flow direction change
HG	hydraulic geodesic
HGI	hydraulic geodesic index
L_i	represents the length of the i-th pipe
$minHG$	the shortest value among all HG
MRI	modified resilience index
$N_{segment}$	total number of segments
N_{val}	number of valve installation
$N_{val,tot}$	total number of valves
$norm$	normalization
$normHGI_{k,s}$	normalized hydraulic geodesic index
$normSHGI$	average of normalized hydraulic geodesic index
$nodes$	total number of demand nodes
$n_{pipe_{segment}}$	number of pipes included in the segment
PDA	pressure-driven analysis
$P_{avg,i}$	average pressure of i-th node
$p_{pipe,i}$	breakage probability for i-th pipe
$p_{segment,s}$	the probability of s-th segment isolation
Rel_{Avg}	average reliability
Rob_i	robustness of i-th node
r_i	breakage rate per length (breaks/ft) for i-th pipe
rel_s	reliability during segment isolation
$sysRob$	system robustness
$Q_{avi,j}$	actual demand (demand output of EPANET)
$Q_{reg,j}$	required demand (base demand input of EPANET)
w_i	weight of the i-th pipe
σ_{P_i}	the standard deviation of pressure at i-th node

References

- Shin, S.; Lee, S.; Judi, D.R.; Parvania, M.; Goharian, E.; McPherson, T.; Burian, S.J. A Systematic Review of Quantitative Resilience Measures for Water Infrastructure Systems. *Water* **2018**, *10*, 164. [[CrossRef](#)]
- Lee, S.; Jung, D. Accounting for Phasing of Isolation Valve Installation in Water Distribution Networks. *J. Water Resour. Plan. Manag.* **2021**, *147*, 06021007. [[CrossRef](#)]

3. Brentan, B.; Monteiro, L.; Carneiro, J.; Covas, D. Improving Water Age in Distribution Systems by Optimal Valve Operation. *J. Water Resour. Plan. Manag.* **2021**, *147*, 04021046. [[CrossRef](#)]
4. Van Den Boomen, M.; Van Mazijk, A.; Beuken, R. First evaluation of new design concepts for self-cleaning distribution networks. *J. Water Supply Res. Technol.—AQUA* **2004**, *53*, 43–50. [[CrossRef](#)]
5. Vreeburg JH, G.; Blokker, E.M.; Horst, P.; Van Dijk, J.C. Velocity-based self-cleaning residential drinking water distribution systems. *Water Sci. Technol. Water Supply* **2009**, *9*, 635–641. [[CrossRef](#)]
6. Hong, S.; Lee, C.; Park, J.; Yoo, D.G. Velocity-based decision of water quality measurement locations for the identification of water quality problems in water supply systems. *J. Korea Water Resour. Assoc.* **2020**, *53*, 1015–1024.
7. Walski, T.M. *Valves and Water Distribution System Reliability*; AWWA National Convention: New York, NY, USA, 1994.
8. Jun, H.; Loganathan, G. Valve-controlled segments in water distribution systems. *J. Water Resour. Plan. Manag.* **2007**, *133*, 145–155. [[CrossRef](#)]
9. Alvisi, S.; Creaco, E.; Franchini, M. Segment identification in water distribution systems. *Urban Water J.* **2011**, *8*, 203–217. [[CrossRef](#)]
10. Giustolisi, O.; Savic, D. Identification of segments and optimal isolation valve system design in water distribution networks. *Urban Water J.* **2010**, *7*, 1–15. [[CrossRef](#)]
11. Kao, J.-J.; Li, P.-H. A segment-based optimization model for water pipeline replacement. *J. Am. Water Works Assoc.* **2007**, *99*, 83–95. [[CrossRef](#)]
12. Shuang, Q.; Liu, Y.; Tang, Y.; Liu, J.; Shuang, K. System reliability evaluation in water distribution networks with the impact of valves experiencing cascading failures. *Water* **2017**, *9*, 413. [[CrossRef](#)]
13. Giustolisi, O. Water distribution network reliability assessment and isolation valve system. *J. Water Resour. Plan. Manag.* **2019**, *146*, 04019064. [[CrossRef](#)]
14. Abdel-Mottaleb, N.; Walski, T. Evaluating segment and valve importance and vulnerability. *J. Water Resour. Plan. Manag.* **2021**, *147*, 04021020. [[CrossRef](#)]
15. Wéber, R.; Huzsvár, T.; Hős, C. Isolation Valve Placement Optimization of Water Distribution Networks to Reduce Vulnerability. *Period. Polytech. Mech. Eng.* **2023**, *67*, 51–58. [[CrossRef](#)]
16. Hernandez, E.; Ormsbee, L. Application of segment based robustness assessment for water distribution networks. In Proceedings of the International Joint Conference in Water Distribution Systems Analysis & Computing and Control in the Water Industry, Kingston, ON, Canada, 23–25 July 2018.
17. Hernandez Hernandez, E.; Ormsbee, L. A Heuristic for Strategic Valve Placement. *J. Water Resour. Plan. Manag.* **2022**, *148*, 04021103. [[CrossRef](#)]
18. Meng, F.; Sweetapple, C.; Fu, G. Placement of isolation valves for resilience management of water distribution systems. In Proceedings of the International Joint Conference in Water Distribution Systems Analysis & Computing and Control in the Water Industry, Kingston, ON, Canada, 23–25 July 2018.
19. Yang, Z.; Guo, S.; Hu, Z.; Yao, D.; Wang, L.; Yang, B.; Liang, X. Optimal Placement of New Isolation Valves in a Water Distribution Network Considering Existing Valves. *J. Water Resour. Plan. Manag.* **2022**, *148*, 04022032. [[CrossRef](#)]
20. Machell, J.; Boxall, J. Modeling and field work to investigate the relationship between age and quality of tap water. *J. Water Resour. Plan. Manag.* **2014**, *140*, 04014020. [[CrossRef](#)]
21. Kang, D.; Lansey, K. Real-time optimal valve operation and booster disinfection for water quality in water distribution systems. *J. Water Resour. Plan. Manag.* **2009**, *136*, 463–473. [[CrossRef](#)]
22. Dias, V.C.; Besner, M.-C.; Prevost, M. Predicting Water Quality Impact After District Metered Area Implementation in a Full-Scale Drinking Water Distribution System. *J. AWWA* **2017**, *109*, E363–E380. [[CrossRef](#)]
23. Boxall, J.B.; Saul, A.J. Modeling Discoloration in Potable Water Distribution Systems. *J. Environ. Eng.* **2005**, *131*, 716–725. [[CrossRef](#)]
24. Husband, S.; Boxall, J. Understanding and managing discoloration risk in trunk mains. *Water Res.* **2016**, *107*, 127–140. [[CrossRef](#)] [[PubMed](#)]
25. Poulin, A.; Mailhot, A.; Periche, N.; Delorme, L.; Villeneuve, J.-P. Planning Unidirectional Flushing Operations as a Response to Drinking Water Distribution System Contamination. *J. Water Resour. Plan. Manag.* **2010**, *136*, 647–657. [[CrossRef](#)]
26. Braga, A.S.; Saulnier, R.; Filion, Y.; Cushing, A. Dynamics of material detachment from drinking water pipes under flushing conditions in a full-scale drinking water laboratory system. *Urban Water J.* **2020**, *17*, 745–753. [[CrossRef](#)]
27. Abraham, E.; Blokker, M.; Stoianov, I. Decreasing the Discoloration Risk of Drinking Water Distribution Systems through Optimized Topological Changes and Optimal Flow Velocity Control. *J. Water Resour. Plan. Manag.* **2018**, *144*, 878. [[CrossRef](#)]
28. Armand, H.; Stoianov, I.; Graham, N. Investigating the Impact of Sectorized Networks on Discoloration. *Procedia Eng.* **2015**, *119*, 407–415. [[CrossRef](#)]
29. Judi, D.R.; McPherson, T.N. *Development of Extended Period Pressure-Dependent Demand Water Distribution Models*; Los Alamos National Lab. (LANL): Los Alamos, NM, USA, 2015.
30. Lee, S.; Jung, D. Shortest-Path-Based Two-Phase Design Model for Hydraulically Efficient Water Distribution Network: Preparing for Extreme Changes in Water Availability. *IEEE Access* **2021**, *9*, 53358–53369. [[CrossRef](#)]
31. Jung, D.; Kang, D.; Kim, J.H.; Lansey, K. Robustness-Based Design of Water Distribution Systems. *J. Water Resour. Plan. Manag.* **2014**, *140*, 04014033. [[CrossRef](#)]

32. Jayaram, N.; Srinivasan, K. Performance-based optimal design and rehabilitation of water distribution networks using life cycle costing. *Water Resour. Res.* **2008**, *44*, W01417. [[CrossRef](#)]
33. Deuerlein, J.; Simpson, A.; Korth, A. Flushing Planner: A Tool for Planning and Optimization of Unidirectional Flushing. *Procedia Eng.* **2014**, *70*, 497–506. [[CrossRef](#)]
34. Beuken, R. *Validation New Design Rules for DWDS: Lab Experiments on Standard Sediment'*; Report Number: BTO 2001.171; Kiwa WR NV: Nieuwegein, The Netherlands, 2001.
35. Blokker, E.M.; Schaap, P.G.; Vreeburg, J.H. Comparing the fouling rate of a drinking water distribution system in two different configurations. In Proceedings of the 11th International Conference on Computing and Control for the Industry Urban Water Management, Exeter, UK, 5–7 September 2011; University of Exeter: Exeter, UK, 2011.
36. Ahn, J.C.; Lee, S.W.; Choi, K.Y.; Koo, J.Y.; Jang, H.J. Application of unidirectional flushing in water distribution pipes. *J. Water Supply Res. Technol.—AQUA* **2011**, *60*, 40–50. [[CrossRef](#)]
37. Armand, H.; Stoianov, I.I.; Graham, N.J.D. A holistic assessment of discolouration processes in water distribution networks. *Urban Water J.* **2015**, *14*, 263–277. [[CrossRef](#)]
38. Creaco, E.; Haidar, H. Multiobjective Optimization of Control Valve Installation and DMA Creation for Reducing Leakage in Water Distribution Networks. *J. Water Resour. Plan. Manag.* **2019**, *145*, 04019046. [[CrossRef](#)]
39. Su, Y.; Mays, L.W.; Duan, N.; Lansley, K.E. Reliability-Based Optimization Model for Water Distribution Systems. *J. Hydraul. Eng.* **1987**, *113*, 1539–1556. [[CrossRef](#)]
40. Creaco, E.; Franchini, M.; Alvisi, S. Evaluating Water Demand Shortfalls in Segment Analysis. *Water Resour. Manag.* **2012**, *26*, 2301–2321. [[CrossRef](#)]
41. Todini, E. Looped water distribution networks design using a resilience index based heuristic approach. *Urban Water* **2000**, *2*, 115–122. [[CrossRef](#)]
42. Morosini, A.F.; Caruso, O.; Veltri, P. Management of water distribution systems in PDA conditions using isolation valves: Case studies of real networks. *J. Hydroinform.* **2019**, *22*, 681–690. [[CrossRef](#)]
43. Islam, M.S. Water Distribution System Failures: An Integrated Framework for Prognostic and Diagnostic Analyses. Ph.D. Thesis, University of British Columbia, Vancouver, BC, Canada, 2012.
44. Corso, P.S.; Kramer, M.H.; Blair, K.A.; Addiss, D.G.; Davis, J.P.; Haddix, A.C. Costs of illness in the 1993 waterborne Cryptosporidium outbreak, Milwaukee, Wisconsin. *Emerg. Infect. Dis.* **2003**, *9*, 426. [[CrossRef](#)]

Disclaimer/Publisher's Note: The statements, opinions and data contained in all publications are solely those of the individual author(s) and contributor(s) and not of MDPI and/or the editor(s). MDPI and/or the editor(s) disclaim responsibility for any injury to people or property resulting from any ideas, methods, instructions or products referred to in the content.